International Journal of Infrared and Millimeter Waves, Vol. 23, No. 11, November 2002 (© 2002)

PRECISION TUNABLE INFRARED SOURCE AT 10 μM: CO_2-LASER/MICROWAVE-SIDEBAND SYSTEM WITH AN EVENSON CO_2 LASER AND A CHEO WAVEGUIDE MODULATOR

Zhen-Dong Sun,[1] R. M. Lees,[1] Li-Hong Xu,[†] M. Yu. Tretyakov,[1,2] and Ivan Yakovlev[2]

[1]*Canadian Institute for Photonic Innovations and Department of Physical Sciences University of New Brunswick Saint John, NB, E2L 4L5, Canada*

[2]*Visiting Scientists from Institute of Applied Physics Russian Academy of Sciences Nizhny Novgorod, Russia*

Received August 20, 2002

Abstract

A CO_2-laser/microwave-sideband tunable infrared source system has been newly built at the University of New Brunswick (UNB) in Canada. The system employs a high-resolution CO_2 laser of Evenson design that lases on a wide range of lines including hot and sequence band lines as well as high-J lines of the regular 9.6 and 10.6 μm bands. The frequency of the CO_2 laser is stabilized to the Lamb dip in the 4.3 μm fluorescence signal in an external CO_2 cell. Microwave (MW) sidebands are generated in a Cheo-type infrared waveguide modulator driven by a synthesized sweeper and a traveling wave tube (TWT) amplifier. The MW sidebands appear on either side of the CO_2 laser line, and are individually separated from the carrier by a tunable Fabry-Perot etalon. The sidebands currently have a typical power of about 1.4 mW and a continuous frequency tuning range of 22 GHz (from ±7 to ±18 GHz) when 5 W laser power and 15 W microwave power are delivered to the modulator. Details are given on the source construction and measured performance characteristics. Features of the source and its planned applications are discussed.

Key words: CO_2 laser, microwave sidebands, Lamb dip, tunable infrared, high-resolution spectroscopy.

[†] to whom all correspondence should be addressed, xuli@unb.ca

I. Introduction

The CO_2 laser is one of the most useful radiation sources in the important mid-infrared region. Many environmental trace gases and large bio-molecules have rich infrared spectra with vibrational fundamental bands lying in the 10 μm region covered by the CO_2 laser lines [1-3]. However, for high-resolution spectroscopy with a normal CO_2 laser, one is generally restricted to accidental close coincidences between CO_2 laser and molecular absorption lines. Such coincidences occur in limited numbers with an essentially random distribution, making systematic studies difficult.

Several years ago, at the Time and Frequency Division of the National Institute of Standards and Technology in Boulder, K. M. Evenson and co-workers developed an improved CO_2 laser design with special mechanical and optical structures [4,5]. By using a ribbed discharge tube and a high-resolution blazed grating, they extended the range of lines of the laser significantly. The new lasers have been used as infrared sources both in spectroscopic studies and as frequency standards [4-6]. Such a CO_2 laser has recently been brought into operation in UNB. It has high resolution and lases not only in the regular bands up to high J of order 50 but also on many hot and sequence band lines. However, because the frequency gap between two adjacent laser lines is of the order of 45 GHz on average, any line-tunable CO_2 laser is still limited for direct spectroscopy to coincidences between the laser lines and the absorption frequencies of interest. Thus, an infrared source with broader frequency tunability and with accurately known frequencies is highly desirable for applications to environmental remote sensing and to spectroscopic studies in a variety of fields.

Such tunable infrared sources (hereafter called CO_2-laser/MW-sideband) appeared some twenty years ago, using the technique of electro-optically modulating the CO_2 laser with tunable microwave radiation in a phase modulator [7, 8]. Two kinds of modulator structures were developed, both driven by a microwave TWT amplifier in the X and Ku MW bands (8 - 12 and 12 - 18 GHz) [7-10] and both of which were used in a multiple resonance spectroscopy experiment on methanol by Xu et al. [11]. Each is an excellent infrared source in terms of tunability, spectral purity, accuracy of synthesized frequency and output power [7-13]. One was developed by P. K. Cheo and co-workers [7], and was constructed from a CdTe-buffered GaAs infrared waveguide with a

traveling-wave micro-strip MW transmission line. The other was developed by G. Magerl and co-workers [8], and consisted of a bulk CdTe crystal filling a microwave cavity operating in a resonant mode. Because the Cheo modulator achieves high efficiency by confining high optical and microwave fields to a very small interaction region, it generates CO_2 laser sidebands over a 20 GHz MW range with powers of several milliwatts. This is more than three times wider in tuning range and one order of magnitude higher in sideband power than the Magerl device. Here at UNB, a Cheo modulator has recently been installed and successfully operated after careful measurement of the input powers and fine adjustment of the alignment to optimize the optical transmission.

With typical CO_2-laser and MW input powers of 10 W and 20 W, respectively, into GaAs waveguide modulators, Cheo et al. [7, 9] and Sun et al. [12, 13] generated CO_2 laser sidebands having powers on the order of several tens of mW and a broadband frequency tuning range of 22 GHz (± 7 - ± 18 GHz). With this infrared source, Cheo et al. measured precise frequencies, relative line strengths, self-broadened Lorentzian linewidths and pressure-induced frequency shifts for eight transitions of NH_3 [9]. However, their CO_2 laser provided limited line coverage in the regular 9 and 10 μm bands, restricting their range of observations. Later, Sun et al. applied a Cheo source to spectroscopic observations of CH_3OH [12,13]. Their main CO_2 laser (Edinburgh Instruments Model PL3) lased on a large number of CO_2 laser lines with high output power (10 – 15 W). Thus, they were able to measure fifty-two excited-state rotational transitions in methanol by IR-MW double resonance with high signal-to-noise ratio [12]. These excited vibrational lines are very weak in ordinary microwave spectroscopy. Later, by using a sub-Doppler Lamb-dip technique, they resolved and observed many transitions in the CO-stretching fundamental band of methanol with a resolution of 0.2 MHz and frequency accuracy of better than 0.20 MHz [13]. However, to reach this high frequency accuracy, they used the beat frequency between the main CO_2 laser and a second reference CO_2 laser which was of Evenson design. In our present tunable CO_2 laser sideband system, we are aiming to obtain a high accuracy directly by using a single Evenson CO_2 laser to drive our Cheo waveguide modulator. In this paper, details of the system constructions and our initial observations are described.

II. Experimental Details and Observations

Fig. 1 shows a block diagram of the experimental setup of our CO_2-laser/MW-sideband tunable infrared source. The infrared radiation from a CO_2 laser is focused into the modulator by lens L1. The frequency of the CO_2 laser is modulated at 1 kHz and stabilized by a synchronous-detector-based servo system which locks the laser to the Lamb dip in the 4.3 μm fluorescence signal from an external CO_2 cell. The MW radiation from a synthesized sweeper is amplified to a power of about 15 W by a broadband TWT amplifier (7 – 18 GHz) and fed to the modulator. The output beam from the modulator contains the two sidebands separated by the MW frequency from the central carrier line, and is collimated by lens L2. The sideband radiation is separated from the carrier using a tunable Fabry-Perot etalon, and is detected by an infrared photodetector. The signal is then displayed either on an oscilloscope or a chart recorder. In the next section, experimental details and observations on the CO_2 laser, the frequency stabilization system, and the generation and separation of the sidebands in our tunable infrared source are described.

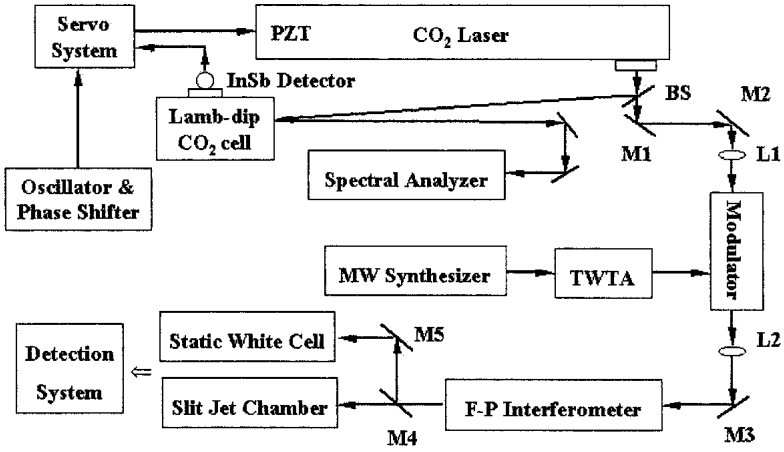

Fig. 1 Block diagram of the experimental setup. BS, beam splitter; L1, L2, ZnSe lenses; M1 - M5, mirrors; TWTA, traveling wave tube amplifier; F-P, Fabry-Perot etalon.

II a. Construction, operation and output spectrum of the CO_2 laser

The construction of the CO_2 laser designed by Evenson and coworkers at NIST Boulder has already been described elsewhere [4,5]. Our laser was also built in the NIST Boulder laboratories. Fig. 2 shows the external connections of our laser system. The laser tube is made of 30 mm OD Pyrex, and is specially designed with cylindrical ribs 1.25 mm deep and approximately 2 mm wide at 15 mm intervals along the entire tube length. These ribs function as apertures, acting to modify the tube mode structure and increase the effective resolution of the diffraction grating. The CO_2 laser gas mixture flows slowly through the inner tube (active length of 1.37 m) and independent discharges are established on each side of the tube via two neon sign cathodes mounted near the centre. A water sleeve around the discharge tube carries cooling water.

The ends of the laser tube are attached by flanges to two aluminum block supports (placed on the grounded honeycomb table) which are connected by three super-invar spacer bars (1.36 m long) to minimize thermal expansion and potential mechanical stresses. At the far end of the laser the mirror plate is mounted via an O-ring to the block support and holds the cylindrical piezoelectric tuning element (PZT) and

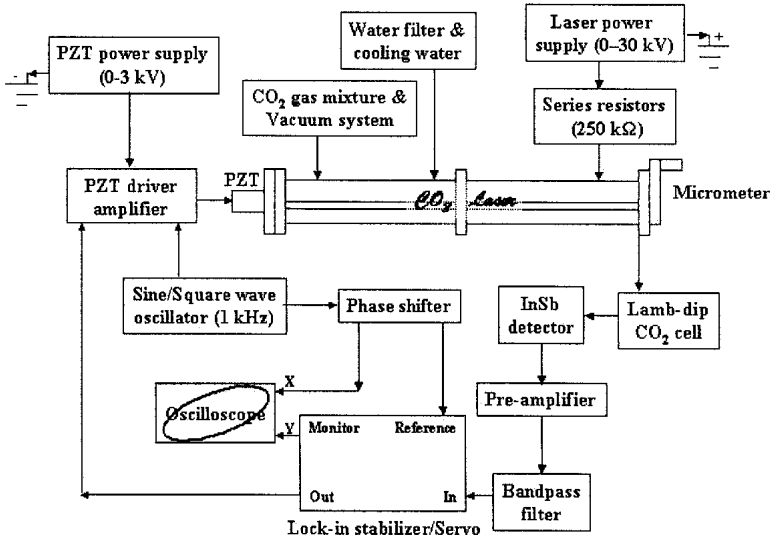

Fig. 2 Frequency stabilization system for the CO_2 laser.

the end mirror. The end mirror is a gold-coated concave mirror of 10 m radius of curvature. At the near end, the grating plate is mounted and holds the grating, two reflecting mirrors and an output window on the outside. The grating (Hyperfine) has 171 lines/mm and is linked to the tuning micrometer (Mitutoyo, 0.001mm resolution) by a spring. The total length of the laser cavity is 1.5 m.

A mechanical pump (Edwards RV3) is used to evacuate the laser discharge tube and maintain the flow of the CO_2 gas mixture through the tube during operation of the laser. Premixed laser gas is used (Air Liquide) consisting of 16.2% N_2, 12% CO_2 and the balance He. To purify the cooling tap water for the laser tube, we use a 20 micron water filter. The negative high voltages for the gas discharges on the two sides of the tube are derived from twin high-voltage current regulators driven from a single power supply (Kilovolt Corp. Model kV30). Voltage is applied to each cathode through a series ballast resistor chain in order to limit the current and to produce a voltage drop to allow simultaneous lighting of both discharges. The two sets of ceramic resistors, each having a total series resistance of 250 kΩ, are mounted in an acrylic resistor box with fan cooling. The laser has a typical warmup time of 30 minutes, and is customarily operated at a total gas pressure of about 12 Torr (1.6 kPa)

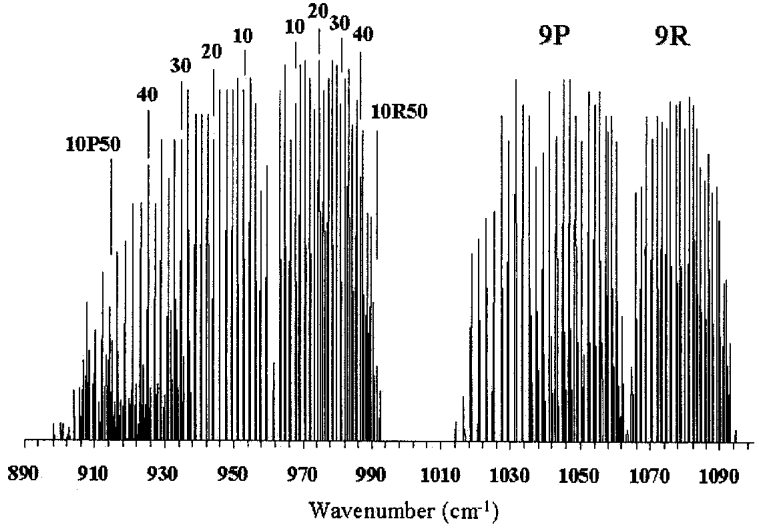

Fig. 3 Observed output line spectrum of the CO_2 laser.

employing a DC bias voltage of 10 kV and a tube current of 10 mA in each leg.

The laser emits linearly polarized radiation (horizontal P) with a spot size of about 5 mm (FWHM) in a Gaussian beam profile. When the micrometer is manually or motor driven to turn the grating, the laser is scanned through its line spectrum. The identification of the output lines is confirmed by a CO_2 spectrum analyzer (Optical Engineering, Inc.). The output power of the laser is measured by a power meter (Coherent Model 201) in order to optimize the gas pressure. So far, we have observed CO_2 laser lines in the ranges 10P(54) - 10P(2), 10R(0) - 10R(50), 9P(50) - 9P(2) and 9R(2) - 9R(50), as well as many hot and sequence band lines. Fig. 3 shows a spectrum of the observed output of the laser versus its oscillation frequency. The typical output powers are 2 W for hot band lines, 7 W and 6 W for regular 9.6 and 10.6 μm band lines, respectively. A zoom-in view of part of the 9P-branch in Fig. 4 shows the positions of the regular, sequence and hot band lines. The energy level diagram of CO_2, shown in Fig. 5(a), illustrates the origin of these transitions in the different bands. The level notation in Fig. 5(a) uses the quantum numbers ν_1, ν_2^{ℓ}, and ν_3 for the symmetric stretching, degenerate bending and asymmetric stretching modes of CO_2, as sketched in Fig. 5(b).

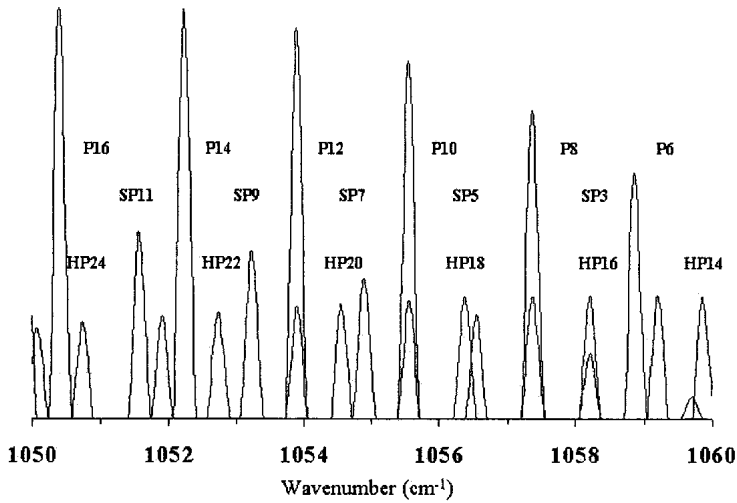

Fig. 4 Zoom-in view of part of the CO_2 laser line spectrum in the 9P branch, showing the regular, sequence band (S) and hot band (H) transitions.

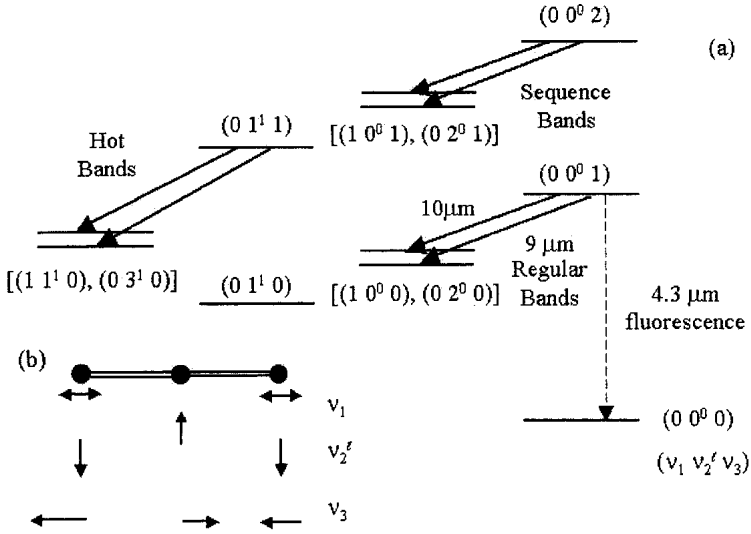

Fig. 5 (a) Energy level diagram of CO_2, (b) Vibrational modes of CO_2 labeled by the quantum numbers ν_1 (symm. stretch), ν_2^ℓ (degenerate bends), ν_3 (asymm. stretch).

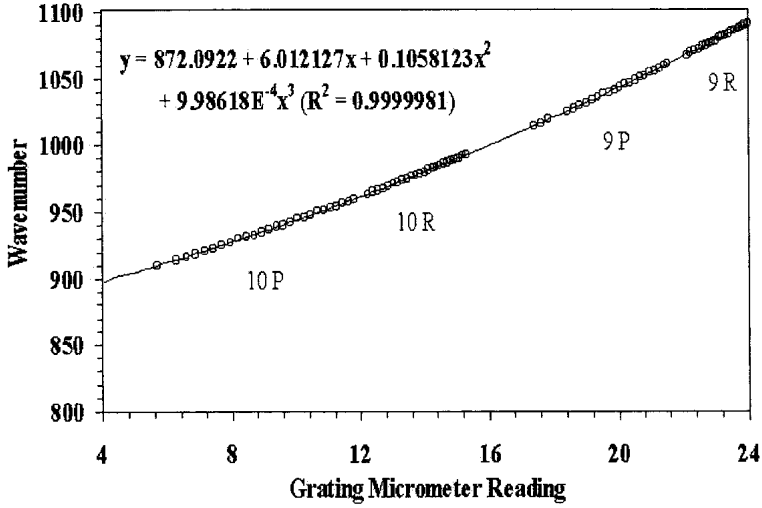

Fig. 6 Relationship of the CO_2 laser oscillation wavenumber to the grating micrometer reading. The solid line is the calibration curve plotted from the displayed equation which represents a polynomial fit to the observations.

As described by Evenson et al. [4] and by Xu et al. [14], the use in this kind of CO_2 laser of a specially blazed grating and a ribbed laser

discharge tube efficiently increases the resolution for the laser lines; this is also seen here from Fig. 3. The relationship of the wavenumbers of the oscillating CO_2 lines to the readings of the grating micrometer is shown in Fig. 6. From this curve, we know the wavenumber coverage of our laser and can easily set a desired laser line according to the grating reading.

II b. CO_2 laser frequency stabilization system

The frequencies of all of the lines in the various CO_2 laser bands have been measured and analyzed by Maki et al. [5] by stabilizing the laser against the saturation dip in the 4.3 μm CO_2 fluorescence (shown as a dashed line in Fig. 5a). In the present work, the fluorescence is generated in a Lamb-dip CO_2 cell containing pure CO_2 at low pressure of about 40 mTorr (5.3 Pa) at room temperature. Input laser power of about 2 W, tapped off the main laser output by a beam splitter as shown in Fig. 1, enters and exits the cell through tilted ZnSe windows and is then reflected back by a plane mirror behind the cell along almost the same path, producing counter-propagating near-parallel beams. The 4.3 μm signal is viewed at right angles to the laser beam through a sapphire

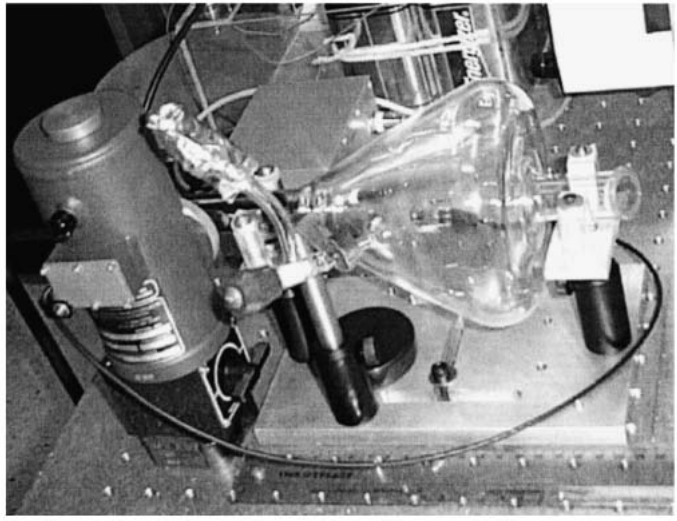

Fig. 7 Layout of the Lamb-dip CO_2 fluorescence cell and InSb detector.

window and detected by a large-area InSb detector (Laser Photonics Model L5911). Fig. 7 depicts our layout and the structure of the CO_2 cell (Allen Glass), which is made from a 1000 ml flask with its neck gold-coated to increase the fluorescence collection efficiency.

With the presence of counter-propagating parallel beams in the cell, a saturated resonance Lamb dip is produced at the centre of the CO_2 absorption line. To allow first-derivative detection of this Lamb dip by the stabilization lock-in amplifier for use as an error-correcting signal, the laser frequency is modulated at 1 kHz by applying a sinusoidal dither voltage to the PZT tuning element. The PZT transducer is a piezoelectric tube onto which the laser end mirror is mounted. The tube forms part of the laser cavity as a continuation from the ribbed glass tube. A sine/square-wave oscillator sends the 1 kHz dither voltage to the PZT driver amplifier, thereby producing a modulation of the laser cavity length and thus the laser frequency. The oscillator incorporates a CG-102R1 resistor-tunable sinewave oscillator chip (NF Corp.), which features excellent frequency and output voltage accuracy using externally connected resistors. A recorder tracing of the 4.3 μm first derivative signal obtained as our laser was swept across the 9P(34) line is shown in Fig. 8. The signal-to-noise ratio for the observed Lamb dip is about 120, while the ratio of the width of the Lamb dip to the CO_2 Doppler width is approximately 1/50.

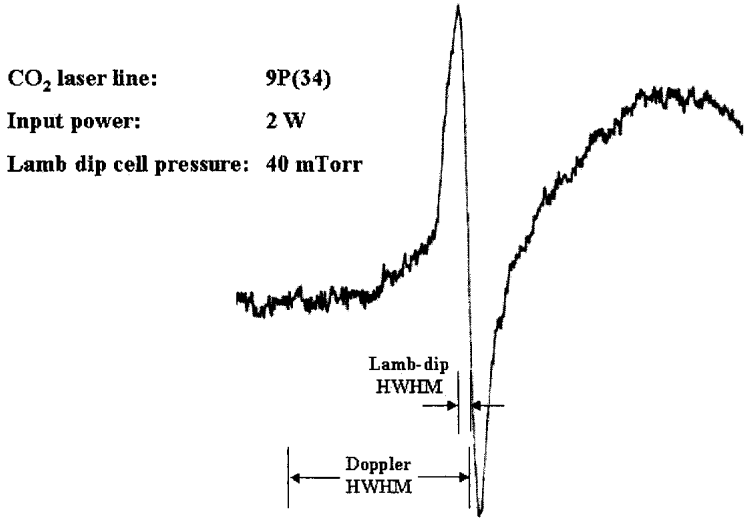

Fig. 8 Recording of the 4.3 μm first-derivative signal obtained from the stabilizer/servo lock-in as the laser frequency is tuned through the centre of the 9P(34) line.

The laser frequency is stabilized by locking the laser to the CO_2 line centre, i.e. to the zero of the Lamb dip first-derivative error signal from the stabilizer lock-in, using a closed feedback loop servo system as shown in Fig. 2. The error signal detected by the InSb detector is pre-amplified, sent through a bandpass filter (0.6 ~ 1.6 kHz) and then demodulated by the stabilizer lock-in. The amplified signal is also monitored prior to demodulation and compared to the 1 kHz dither voltage to allow visual observation of the Lamb dip as a Lissajous ellipse on an oscilloscope in X-Y mode. The stabilizer lock-in output is fed to a PZT driver amplifier where it is applied in series with the positive PZT high voltage (0 - 1.2 kV, supplied by Power Designs Model 1570) to the laser PZT modulating element in order to control the length of the laser cavity and thereby the laser frequency. With this locking system, the frequency uncertainty of our stabilized CO_2 laser is estimated to be a few tens of kHz.

II c. Sideband generation, separation and observation

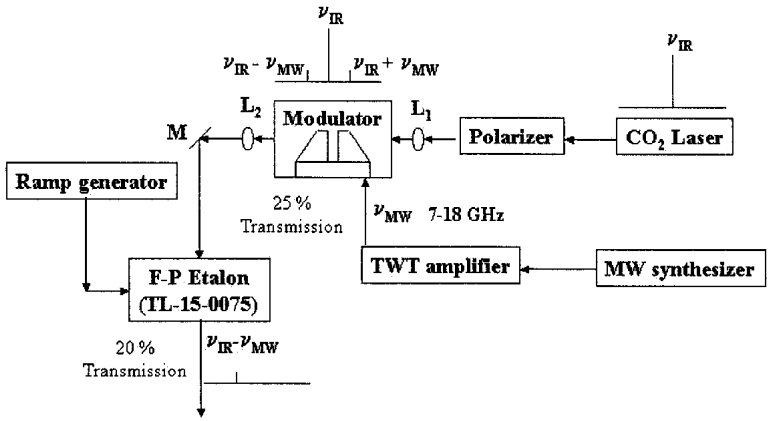

Fig. 9 Schematic diagram for the generation, separation and observation of the tunable CO_2-laser/MW-sidebands. (Overall % transmission efficiency can still be increased with improved alignment and additional optics).

Fig. 9 shows the schematic diagram for the generation, separation and observation of the tunable CO_2 laser sidebands. The structure, design parameters and fabrication procedure of the Cheo-type microwave-tuned waveguide modulator (PC Photonics) have been described in detail

previously in Ref. 7. The waveguide modulator is a traveling-wave device, which operates in the X and Ku bands. Our unit is shown in Fig. 10, mounted on the 5-dimensional kinematic stage required for precise positioning and angular alignment. It consists of a CdTe-buffered GaAs thin-slab optical waveguide 3.5 cm long and having a total thickness of 25 μm. A microwave microstrip transmission line is deposited to the top surface of the slab waveguide. At the input and the output of the transmission line, a three-quarter-wave impedance transformer network is fabricated into the waveguide to obtain a flat broadband frequency response [7]. The laser beam is coupled into and out of the waveguide by two anti-reflection-coated right-angle Ge prisms. Since there is significant thermal dissipation from the high microwave and laser powers, the whole

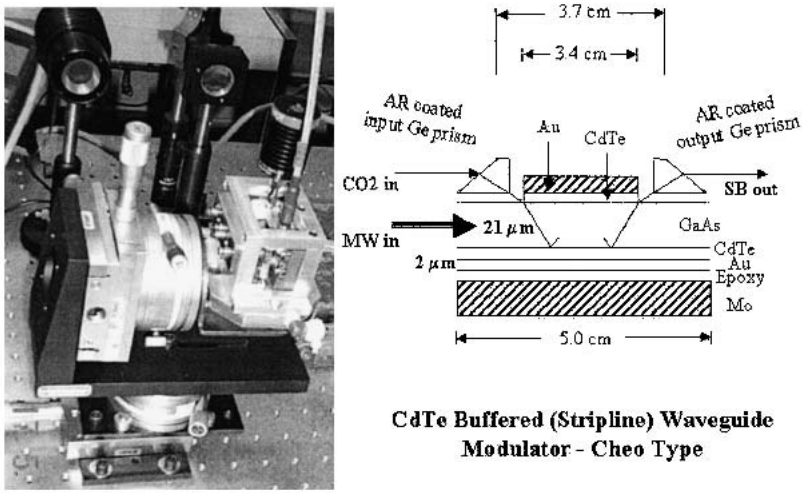

Fig. 10 Photographic view of the Cheo waveguide modulator mounted on a 5-dimensional kinematic stage, with schematic diagram of the modulator.

aluminum modulator housing body is water-cooled.

In order to orient the polarization of the laser radiation parallel to the plane of the GaAs waveguide, a two-mirror arrangement is used to rotate the horizontally polarized beam from the laser into the vertical direction. To optimize the diffraction-limited beam diameter at the entry surface of the front Ge prism, starting from our input CO_2 laser beam size, we selected a ZnSe lens with a focal length of 10" to transmit the

laser beam through the 1-mm-wide waveguide channel. After careful adjustment of the laser beam path and the modulator positioning, we obtained a coupling efficiency of 25% through the modulator for an input laser power of 5 W. The transmitted output beam from the modulator was point-like, with a somewhat elliptical shape, and was then collimated by a second 10" focal length ZnSe lens.

To generate the MW radiation over the 7 - 18 GHz operating range of the modulator, we employ a synthesized sweeper (83630A, 10 MHz - 26.5 GHz, Hewlett Packard). The low power output from this synthesizer is then amplified in a travelling-wave tube amplifier (CPI Model ZM-6991K4ADI) up to levels of 5 - 20 W. The TWT output is connected to the MW input port of the modulator by a 1-m low-loss coaxial cable, and a 20-W matched load is connected to the exit port. Because the gain of the TWT amplifier varies across its operating frequency range, it is necessary to use different drive levels from the synthesizer to achieve the desired MW output power of order 15 W from the TWT amplifier at the different frequencies. We measured the TWT output for a range of input powers and frequencies and checked the test data provided by the CPI customer service division. We then obtained a gain transfer curve giving the required synthesizer output power as a function of microwave frequency, shown in Fig. 11.

In our initial trials to obtain the CO_2 laser sidebands, the 9P(34)

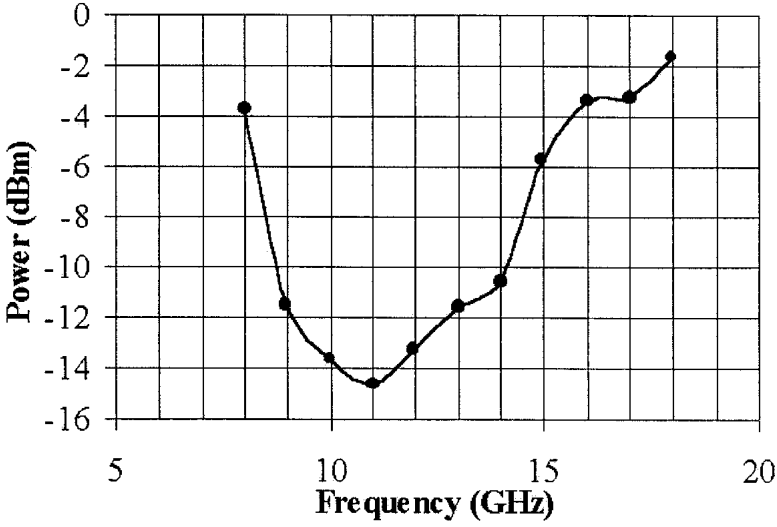

Fig. 11 Gain transfer curve showing the frequency variation in the synthesizer output power required to obtain 15 W output from the TWT amplifier.

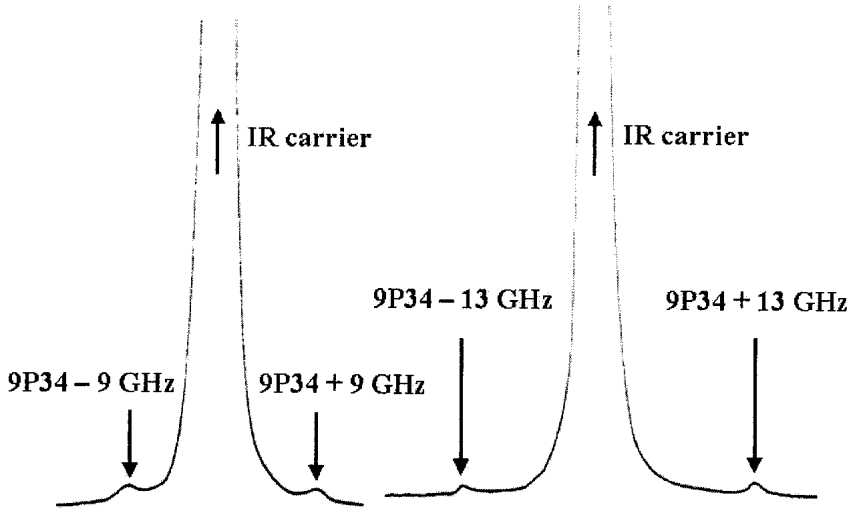

Fig. 12 Spectra of the CO_2 laser sidebands at the output of the F-P etalon for microwave frequencies of 9 and 13 GHz, recorded with a lock-in amplifier time constant of 0.3 s.

CO_2 laser line at 1033.4879917 cm^{-1} was selected and the MW synthesizer tuned to a frequency of 9 GHz. The inputs to the modulator were set at a microwave power of 15 W and a laser power of 5 W. For monitoring the two sidebands and separating them from the carrier in the output of the modulator, a tunable Fabry-Perot etalon (Burleigh TL-15-0075) and a pyroelectric infrared photodetector were used. While sweeping the etalon tuning voltage (0 - 1 kV) from a ramp generator (Burleigh RG-93) over one free spectral range (75 GHz), we recorded the output spectrum to look for the CO_2 laser sidebands.

Fig. 12 shows the results for the 9P(34) line, recorded using an optical chopper, a lock-in amplifier time constant of 0.3 s, laser power of 5 W and MW power of about 15 W. Spectra were taken using microwave frequencies of both 9 and 13 GHz, and the displacements of the upper and lower sidebands away from the 9P(34) carrier can be clearly seen in the recordings. The overall carrier to sideband conversion efficiency (P_s/P_c) was measured to be about 0.55% for each sideband. This translates to a sideband power of approximately 1.4 mW given the modulator and F-P etalon transmission efficiencies of 25% and 20%, respectively. In subsequent observations of the laser sidebands over the full frequency range, with a power of 5 W in the 9P(34) laser line, we obtained the sideband detector voltages and efficiencies shown in Table 1.

Table 1. Observed sideband output with the 9P(34) CO_2 laser line[a]

MW Freq. (GHz)	P_{syn}[b] (dbm)	TWT Gain[c] (db)	P_{TWT}[d] (W)	SB Signal[e] (mV)	SB Efficiency[f] (%)
7	-2.0			3	
8	-6.0	46.8	12.0	3	0.27
9	-12.0	54.5	17.8	6	0.55
10	-14.0	56.7	18.6	4	0.36
11	-14.0	57.7	23.4	6	0.55
12	-12.0	56.3	26.9	5	0.45
13	-10.0	54.6	28.8	5	0.45
14	-9.0	53.6	28.8	5	0.45
15	-5.0	48.8	24.0	4	0.36
16	-3.0	46.4	21.9	5	0.45
17	1.2	46.3	[56.2]	1.5	[0.14]
18	3.0	44.7	[58.9]	0.1	[0.01]

[a] Input laser power to the modulator was 5 W.

[b] Input power level to the TWT amplifier as set on the microwave synthesizer.

[c] Gain values of our TWT amplifier, as supplied by the manufacturer.

[d] Output power from the TWT amplifier, calculated from P_{syn} and the TWT gain. The values at 17 and 18 GHz are clearly too high, and the TWT was probably saturated.

[e] Peak sideband signal measured on a pyroelectric detector at the output of the F-P etalon. The corresponding signal due to the central carrier was 1.10 V at all frequencies. A SB signal of 6 mV equates to a SB power of approximately 1.4 mW.

[f] Conversion efficiency for a single sideband, calculated as the SB signal from the detector divided by the central carrier signal level of 1.10 V. Values at 17 and 18 GHz are anomalous.

Here, P_{syn} refers to the synthesizer output setting and P_{TWT} to the output of the TWT amplifier as calculated from the amplification values supplied by the manufacturer for our tube. The actual power at the modulator would be slightly reduced due to the attenuation in the 1-m length of low-loss coupling cable. The P_{TWT} values at 17 and 18 GHz are clearly too high, and the TWT was probably saturated at approximately 16 W output according to its specifications. The conversion efficiency is reasonably uniform at around 0.5% over the 7 – 16 GHz band, but the detector output drops sharply at 17 and 18 GHz. We are investigating the possibility that this might be due to a standing wave "hole" in the MW transmission towards the high frequency end of the band, which could also be associated with the anomalous P_{TWT} values.

III. Discussion and Conclusions

The CO_2 laser sideband system is a very convenient tunable coherent infrared source. The laser itself has many emission lines and the microwave sidebands can be tuned over a range of 22 GHz (±7 – ±18 GHz) between adjacent lines, which are separated on average by a gap of order 45 GHz for the main bands. With the hot band and sequence band lines as well, the overall frequency coverage approaches 80% of the region from 900 to 1100 cm^{-1}, and could be even more with the use of isotopic CO_2 lasers over the region from 800 to 1100 cm^{-1}. The frequency accuracy is high because the MW synthesizer has excellent precision and could in fact be used as a microwave calibrator while the laser is tightly locked to the narrow Lamb dip in the 4.3 μm fluorescence signal. (Experiments to determine the absolute frequency accuracy of the locked source are currently in progress.) Determination of the sideband frequency is easy because the laser carrier frequency is precisely known and then one needs simply to add or subtract the MW synthesizer frequency. Thus, the CO_2 sideband system represents a powerful tool for spectroscopic investigations in the 10 μm region, where many important vibrational fundamentals occur. The source output power is substantially higher than lead-salt tunable diode lasers (TDL), the other common spectroscopic source in that same wavelength region.

In terms of the separation of the microwave sidebands from their carrier, at the present stage we use a scanning Fabry-Perot etalon whose specifications and alignment relative to the beam transmitted from the modulator essentially determine the sideband output power and frequency purity. The free spectral range (FSR) of our Burleigh F-P interferometer is 75 GHz; its finesse (F) and transmission efficiency (T) according to the manufacturer should be given by the relations

$$F = -5S + 85 \qquad \text{and} \qquad T = -2S/30 + 0.9$$

where S is the beam size (in mm). Because the carrier power is high, with a typical ratio of 200:1 relative to the sidebands for our system at present, it is hard to eliminate the carrier completely by a F-P interferometer having a finesse of less than 30 [7]. Thus, further improvements to reduce the incident beam size to the F-P etalon are desirable, and we are exploring the use of concave focusing mirrors at various points in the beam path. As well, because the sideband output power is proportional to laser power for given microwave input to the modulator [7], we are looking to increase the laser power up to the 10 - 15 W range by raising

the tube discharge current and CO_2 gas pressure, in order to optimize the sideband output.

In conclusion, we have constructed a tunable infrared source in which microwave sidebands are added to CO_2 laser carrier lines with an overall conversion efficiency of approximately 0.5%. With this source, high-resolution spectroscopic studies within frequency windows from 7 - 18 GHz on either side of each CO_2 line can be carried out on molecular gas samples. As shown in Fig. 1, we currently have an 0.6-m White-type multipass absorption cell of optical path length up to 12 m as well as a new slit-jet molecular beam absorption chamber with multipass optics nearing completion in our laboratory. With this instrumentation, we will be able to carry out a wide variety of studies on important stable molecules as well as transient species and weakly bound van der Waals complexes. Initially, we intend to investigate static cell and slit-jet gas phase spectroscopy for molecules of environmental and atmospheric relevance such as ammonia, methanol, and OCS as well as large environmental and bio-molecules (e.g. HFC's, toluene and gasoline), both for monomers and weakly interacting van der Waals clusters.

Acknowledgements

We are grateful to Messrs. T. Kelly, W. Armstrong, C. Boone, K. Q. Liu and Dr. C. J. Hsu for technical assistance. Financial support of this research by the Canadian Institute for Photonic Innovations and the Natural Sciences and Engineering Research Council of Canada is gratefully acknowledged. M.Y.T. acknowledges support from RFBR Grant No. 00-02-16604 and the Russian Ministry of Sciences and Technologies.

References

1. F.R. Petersen, D.G. McDonald, J.D. Cupp, and B.L. Danielson, Phys. Rev. Lett. 31, 573 (1973).
2. C. Freed and A. Javan, J. Appl. Phys. 17, 53 (1970).
3. K.M. Evenson, D.A. Jennings, and F.R. Petersen, J. Appl. Phys. 46, 576 (1984).
4. K.M. Evenson, C.-C. Chou, B.W. Bach, and K.G. Bach, IEEE J. Quantum Electron. 30, 1187 (1994).

5. A.G. Maki, C.-C. Chou, K.M. Evenson, L. Zink, and J.-T. Shy, J. Mol. Spectrosc. 167, 211 (1994).
6. F. Matsushima, H. Odashima, D. Wang, S. Tsunegawa, and K. Takagi, Japan. J. Appl. Phys. 33, 315 (1994).
7. P.K. Cheo, IEEE J. Quantum Electron. QE-20, 700 (1984).
8. G. Magerl, W. Schupita, and E. Bonek, IEEE J. Quantum Electron. QE-18, 1214 (1982).
9. P.K. Cheo, Z. Chu, L. Chen, and Y. Zhou, Appl. Opt. 32, 836 (1992).
10. G. Magerl, J.M. Frye, W. Kreiner, and T. Oka, Appl. Phys. Lett. 42, 656 (1983).
11. L.-H. Xu, A.M. Andrews, and G.T. Fraser, J. Chem. Phys. 103, 14 (1995).
12. Z.D. Sun, F. Matsushima, S. Tsunekawa, and K. Takagi, J. Opt. Soc. Am. B 16, 1447 (1999).
13. Z.D. Sun, F. Matsushima, S. Tsunekawa, and K. Takagi, J. Opt. Soc. Am. B 17, 2068 (2000).
14. L.-H. Xu, R.M. Lees, K.M. Evenson, C.-C. Chou, J.-T. Shy, and E.C.C. Vasconcellos, Canad. J. Phys. 72, 155 (1994).